INTERNATIONAL JOURNAL OF CLIMATOLOGY
Int. J. Climatol. **36**: 4815–4830 (2016)
Published online 8 February 2016 in Wiley Online Library
(wileyonlinelibrary.com) DOI: 10.1002/joc.4671

RMetS
Royal Meteorological Society

Interannual variability of heat waves in South Korea and their connection with large-scale atmospheric circulation patterns

Woo-Seop Lee[a] and Myong-In Lee[b]*

[a] *Climate Research Department, APEC Climate Center, Busan, Republic of Korea*
[b] *School of Urban and Environmental Engineering, Ulsan National Institute of Science and Technology, Ulsan, Republic of Korea*

ABSTRACT: This study investigates the interannual variation of heat wave frequency (HWF) in South Korea during the past 42 years (1973–2014) and examines its connection with large-scale atmospheric circulation changes. Korean heat waves tend to develop most frequently in late summer during July and August. The leading Empirical Orthogonal Function accounting for 50% of the total variance shows a mono-signed pattern over South Korea, suggesting that the dominant mechanisms responsible for the heat wave are linked in a spatial scale much larger than the nation. It also exhibits a regional variation with more occurrences in the southeastern inland area. The regression of the leading principal component (PC) time series of HWF with large-scale atmospheric circulation identifies a north–south dipole pattern between the South China Sea and Northeast Asia. When this large-scale circulation mode facilitates deep convection in South China Sea, it tends to weaken moisture transport from the South China Sea to Northeast Asia. Enhanced deep convection in the South China Sea triggers a source of Rossby wave train along southerly wind that generates positive geopotential height anomalies around Korea. The anomalous high pressure pattern is accompanied by large-scale subsidence in Korea, thereby providing a favourable condition for extreme hot and dry days in Korea. This study highlights that there is a decadal change of the relationship between Korean heat waves and large-scale atmospheric circulation patterns. The tropical forcing tends to be weakened in the recent decade, with more influences from the Arctic variability from the mid-1990s.

KEY WORDS heat wave frequency; South Korea; interannual variability; atmospheric circulation

Received 24 May 2015; Revised 21 October 2015; Accepted 4 January 2016

1. Introduction

Extreme weather events, such as heat waves, are receiving more attention in recent years, due to their severe damage to the society and terrestrial ecosystems (WMO, 2011; Coumou and Rahmstorf, 2012). For example, high mortality is associated with the frequent occurrence of heat waves, as well as with other natural disasters such as typhoons and floods in South Korea from 1901 to 2008 (Kysely and Kim, 2009). During the summer of 1994, East Asia including southern Korea, Japan, and central China suffered from the worst heat wave, which resulted in at least 3384 heat-related victims in South Korea alone (Kysely and Kim, 2009). This was an unprecedented record-breaking event which had 29 consecutive days of a daily maximum temperature exceeding 33 °C. There have been studies indicating the increase of severe heat wave events in recent decades (e.g. Easterling *et al.*, 2000). It is *likely* that the heat wave frequency (HWF) has increased in Europe, Asia, and Australia since 1950 according to the assessment by IPCC (2013). Heat waves are expected to be more frequent and intensified in magnitude in the future due to global warming (Meehl and Tebaldi, 2004; Christidis *et al.*, 2005; Hansen and Sato, 2012; Coumou and Robinson, 2013; Watanabe *et al.*, 2013). The level of assessment by IPCC is *very likely* in late 21st century. An understanding of the dynamical and physical processes related to heat waves is crucial in improving our ability to predict the phenomenon and develop an adaptation strategy for related health issues and agricultural production.

Although climate model results show that the frequency, intensity and duration of heat waves in the future will increase, the changes will not be distributed evenly in space but they will be affected by the changes in large-scale atmospheric circulation pattern (Meehl and Tebaldi, 2004). The occurrence frequency of temperature extremes has dramatically changed in the past few decades, for which we cannot exclude global warming (IPCC, 2013) and the associated large-scale pattern changes as the possible causes (Christidis *et al.*, 2005; Wen *et al.*, 2013). The relationship between the occurrence of extreme temperature and the large-scale atmospheric circulation pattern has been extensively studied at the global and regional scales (Chen and Newman, 1998; Kenyon and Hegerl, 2008; Scaife *et al.*, 2008; Schubert *et al.*, 2011; Teng *et al.*, 2013; Watanabe *et al.*, 2013, and many). For example, Chen and Newman (1998) and Schubert *et al.* (2011) suggested the important role of the formation of the quasi-stationary Rossby waves that precede the occurrence of severe heat waves in North

* Correspondence to: M.-I. Lee, School of Urban and Environmental Engineering, Ulsan National Institute of Science and Technology, 50 UNIST-gil, Ulju-gun, Ulsan 698-798, Republic of Korea. E-mail: milee@unist.ac.kr

America. Based on model results using many ensemble atmospheric model simulations, Teng *et al.* (2013) suggested that severe heat waves in the United States can be driven purely by mid-latitude internal dynamics of atmosphere, which trigger the planetary Rossby waves trapped in the mid-latitude with a wavenumber 5 structure. They further discussed that the wavenumber-5 pattern is likely to be a physical mode on subseasonal timescales, both observed and simulated in a model, and it has little connection with the tropical diabatic forcing.

The previous studies emphasizing the role of mid-latitude dynamics (e.g. Teng *et al.*, 2013), however, do not entirely exclude the possible influences from the changes in large-scale diabatic heat source either in tropics or high-latitudes. This must be particularly relevant in explaining the mechanisms of the interannual variability in the occurrence frequency and intensity changes of severe heat waves, although the development and maintenance of severe heat waves are largely affected by the quasi-stationary Rossby waves in short-term subseasonal variability. A large heat source in the Indo-Pacific warm pool region can be a source of large-scale Rossby waves that emanate from the tropics and propagate into the extratropics, which is also subject to the variability in interannual time scale of ENSO and Asian summer monsoon (Ding and Wang, 2005; Wang *et al.*, 2009; Ding *et al.*, 2011; Lee *et al.*, 2013; Moon *et al.*, 2013). The studies of Ding and Wang (2005) and Moon *et al.* (2013) showed that the atmospheric teleconnection patterns are quite distinctive between El Nino and La Nina. Nitta (1987) found out that a linkage between anomalous convection over the tropical western North Pacific and the large-scale atmospheric circulation over East Asia in summer, so-called the Pacific-Japan (PJ) teleconnection pattern. Wang *et al.* (2001) demonstrated that the circulation changes associated with an enhanced western North Pacific summer monsoon (WNPSM) can lead to deficient rainfall over East Asia and the Great Plains of the United States. On the other hands, the weak WNPSM suppresses the convection over western North Pacific and transports moisture to the East Asia region, thus forming a dipole-like anomalous rainfall pattern. This dipole pattern is characterized by zonally elongated anticyclone pattern along 35°N and the cyclone along 20°N in the subtropical WNP. This pattern is also known to be closely linked to the tropical Indian Ocean Sea surface temperature (SST) (Yang *et al.*, 2007; Li *et al.*, 2008; Wu *et al.*, 2009). Through these mechanisms, the changes in South Asian summer monsoon circulation can cause either extremely hot or wet condition in East Asia.

Atmospheric teleconnection patterns are also linked with the large-scale blocking patterns in mid-latitudes. Nakamura and Fukamachi (2004) suggested that the blocking episodes related to the variability of the Okhotsk high strongly impact the mid-summer temperature extremes in East Asia. Park and Schubert (1997) investigated the abnormally warm temperature condition in Korea in 1994, and suggested an important role of the large-scale atmospheric circulation pattern change driven by the interaction between orography and zonal wind over the Tibetan Plateau.

Tang *et al.* (2014), on the other hand, suggested the important role of the Arctic climate variability in developing extreme hot days in the Northern Hemisphere summer. They indicated that the decrease of sea and land ice extent in the Arctic tends to weaken upper-level jet stream and shift its position to north, serving as a mechanism for tropical weather and the frequent occurrence of persistent hot days over mid-latitude continents. As suggested, a pronounced variability in the Arctic sea ice extent can serve as a large-scale diabatic heat source, affecting the mid-latitude teleconnection patterns significantly through its ice-albedo feedback in interannual timescale. Moreover, the Arctic sea ice extent has experienced a rapid decline in the recent summers with increased interannual variability (Serreze *et al.*, 2007; Stroeve *et al.*, 2012; Kang *et al.*, 2014a), speculating that the influences from the Arctic on the mid-latitude weather and climate variability should be non-stationary and have long-term changes.

Specifically focusing on the area of Korean peninsula and the vicinity, the present study investigates the interannual variation of the HWF and its connection with the large-scale atmospheric circulation pattern over East Asia in more detail using multi-year observations. Long-term statistics based on data over 42 years (1973–2014) exhibit robust relationships between Korean HWF and large-scale atmospheric circulation patterns, as well as the changes in the relationship between the decades. Linear regression analysis between HWF and large-scale atmospheric and surface variables has been conducted, particularly examining the influences of diabatic heat source from the tropics and the Arctic in boreal summer. We further discuss relevant dynamical mechanisms in an effort to explore the potential predictors and to increase the current prediction capability for the extreme temperature events.

2. Data and methodology

This study analysed surface temperature observation data for July–August, when the heat wave event occurs most frequently in South Korea during these months (as will be discussed in Section 3 with Figure 2). Figure 1(a) shows the topography distribution in East Asia and the geographical location of South Korea, over which the heat wave analysis has been conducted. The daily maximum surface temperature data are provided without missing values by the Korea Meteorological Administration (KMA) for 60 weather stations from 1973 to 2014 (Figure 1(b)). The National Centers for Environmental Prediction (NCEP) and National Center for Atmospheric Research (NCAR) reanalysis version 1 data (NCEP/NCAR-1) in 2.5° latitude by 2.5° longitude horizontal resolution were also used to characterize the large-scale atmospheric circulation pattern (Kalnay *et al.*, 1996). The variables in the analysis include the monthly-mean 2-m temperature, geopotential height (GPH), sea-level pressure (SLP), humidity and zonal and meridional winds. It is known

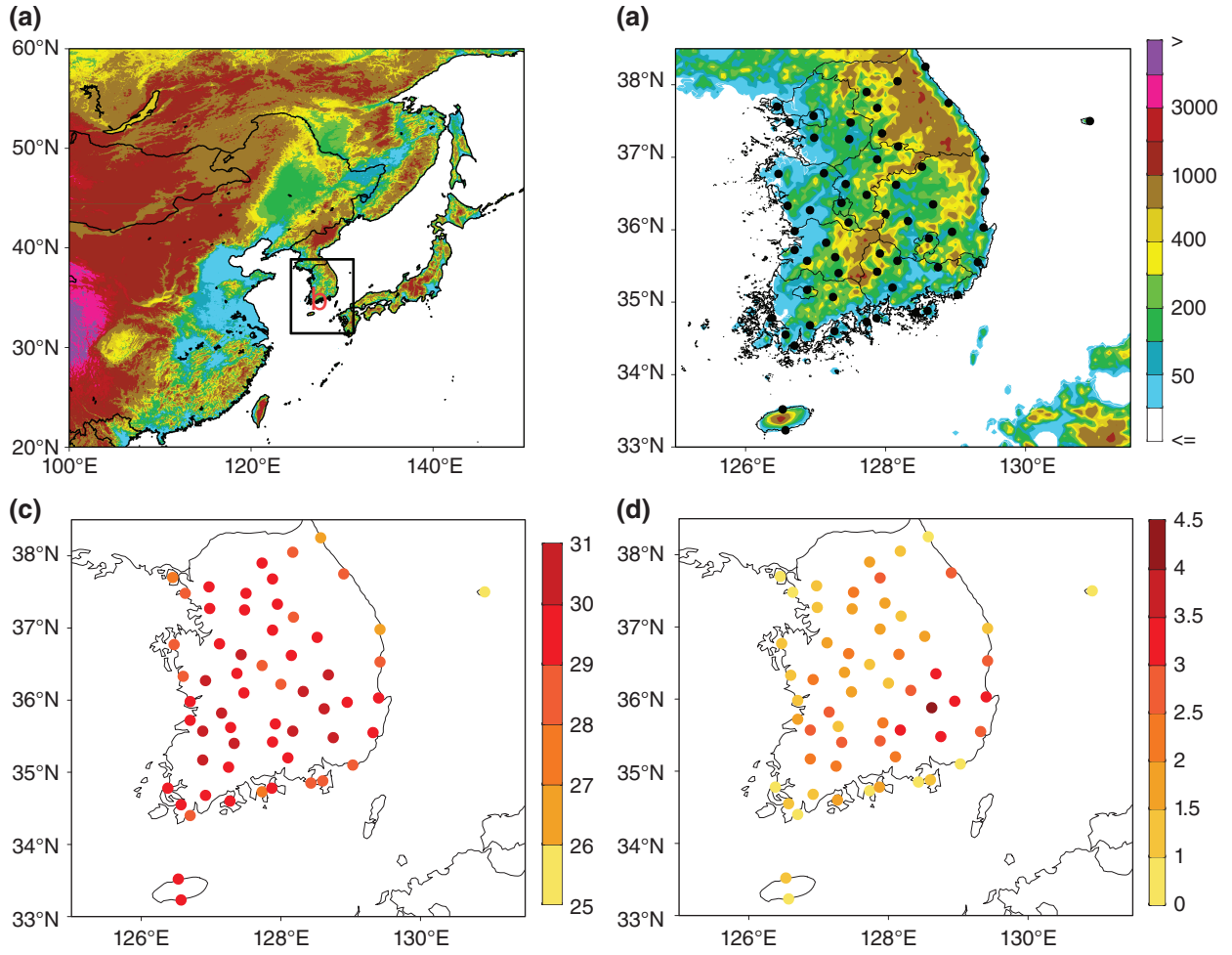

Figure 1. (a) Geographical location of South Korea, (b) the location of 60 weather stations for the heat wave analysis (solid circle), (c) climatological-mean (1973–2014) distribution of daily maximum surface temperature (°C), and (d) climatological-mean heat wave frequency (unit: number of occurrence) during July to August. Shaded is the surface elevation above sea level (unit: m) in (a) and (b).

that NCEP/NCAR-1 has the data discontinuity before and after 1979 by the inclusion of satellite data (Sturaro, 2003). However, we found that this does not modify the large-scale patterns qualitatively in our regression analysis. In Section 3, we analysed the SLP data to investigate the possible impacts from the Arctic on large-scale circulation over East Asia. In spite of the data uncertainty in the Arctic (e.g. Lindsay *et al.*, 2014), we found that the Arctic Oscillation (AO) pattern and associated time series are not sensitive to the choice of atmospheric reanalysis data currently available. We used the monthly mean outgoing longwave radiation (OLR) obtained from the NCEP Climate Prediction Center (Trenberth *et al.*, 2002), and NOAA extended reconstructed sea surface temperature (ERSST) version 3 (Smith *et al.*, 2008).

The KMA defines the heat wave event if there is a period of at least two consecutive days whose daily maximum temperature ($T^{\max}$) exceeds 33 °C. The threshold of 33 °C corresponds to the 90th percentile of daily maximum summertime temperature in Korea. This study defines the HWF as the total number of heat wave events at each station from July to August. In this calculation, any consecutive days of $T^{\max}$ exceeding 33 °C are counted as one heat wave event regardless of its duration. In Section 3.1, we compare this index with other quantitative measures such as the heat wave duration (HWD) and the intensity (HWI) indices. HWD is defined as:

$$\mathrm{HWD} = \frac{1}{n}\sum_{j}^{n} \mathrm{I}\left(T_j^{\max} \geq 33\ ^{\circ}\mathrm{C}\right) \tag{1}$$

where $T_j^{\max}$ indicates the daily maximum temperature at day j, and the indicator function $\mathrm{I}(\cdot) = 1$ if the argument is true and is zero otherwise. In Equation (1), $n = 62$ is the number of days during September to August. The values are the sum of the cases when the daily maximum temperature exceeds 33 °C. HWI is defined as:

$$\mathrm{HWI} = \frac{1}{n}\sum_{j}^{n}\left(T_j^{\max} - 33\ ^{\circ}\mathrm{C}\right), \quad \text{where} \quad T_j^{\max} \geq 33\,^{\circ}\mathrm{C}. \tag{2}$$

In Section 3.1, we identified the dominant spatial pattern of HWF over Korea using the Empirical Orthogonal Function (EOF) analysis. In Section 3.2, the regression analysis was then applied on the principal component (PC) time series to identify the connection with large-scale atmospheric variables.

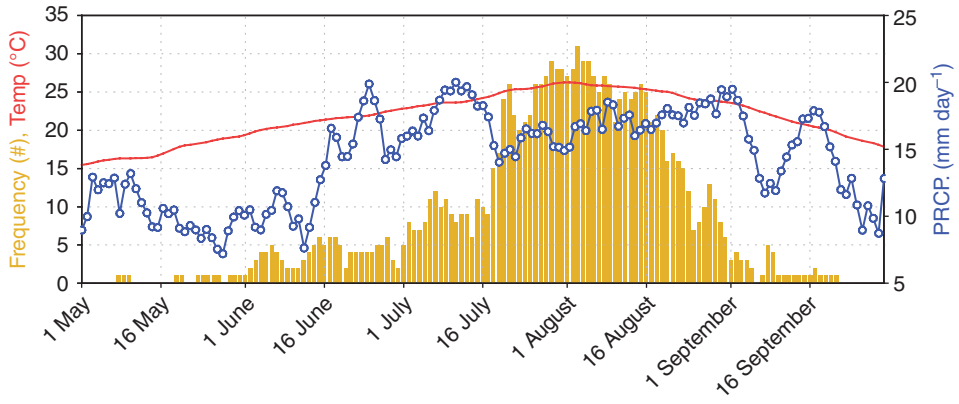

Figure 2. Occurrence frequency of the hot day (bar graph) in South Korea from May to September for the past 42 years (1973–2014). The value is the sum of the cases when the daily maximum surface temperature exceeds 33 °C and the sum of stations meeting this criterion among the 60 weather stations. Also presented are the daily-mean precipitation (blue line with open circle) and surface temperature (red line) averaged over the 42 years.

3. Results

3.1. Interannual variability of HWF in Korea

Figure 1(c) and (d) shows climatology of daily maximum temperature and HWF in South Korea during July to August, respectively. Two patterns are apparently different, suggesting that the occurrence frequency of heat wave in South Korea is not entirely connected with the magnitude of time-averaged daily maximum temperature. A prominent feature is the high values over the southeastern inland area. This region has basically higher values in the climatological-mean daily maximum temperature and also less precipitation during summer. This suggests that the regional variation of HWF is complicatedly affected by factors such as continentiality (i.e. distance from the sea), time-mean daily maximum temperature, and precipitation amount. There have been studies using observational analysis and climate models, which indicate that a deficit in soil moisture can lead to more frequent and severer heat waves (e.g. Dai *et al.*, 1998; Hirschi *et al.*, 2010; Alexander, 2011). Figure 2 shows the total number of hot days ($T_{i,j}^{\max} \geq 33$ °C) in South Korea each day from May to September for the past 42 years from 1973 to 2014. Also presented are the daily-mean precipitation and 2-m temperature averaged over the same period. The frequency of hot days shows a clear seasonal variation peaking in summer, particularly pronounced during mid-July to August. Note that although this time is coincident with the peak time of the daily-mean surface temperature, the frequency of hot days is not necessarily coincident with the mean temperature increase alone. In a climatological-mean sense, the probability of heat waves increases sharply after the wet period of the East Asia summer monsoon in Korea (a.k.a. Changma), which rainfall comes typically from mid-June to mid-July (Choi *et al.*, 2012). Although there is also the chance for heat waves in June and September, we restrict our analysis of heat wave days to the months from July to August.

In Figure 3, we compare the interannual variation of the three heat wave indices (HWF, HWD, and HWI) for the

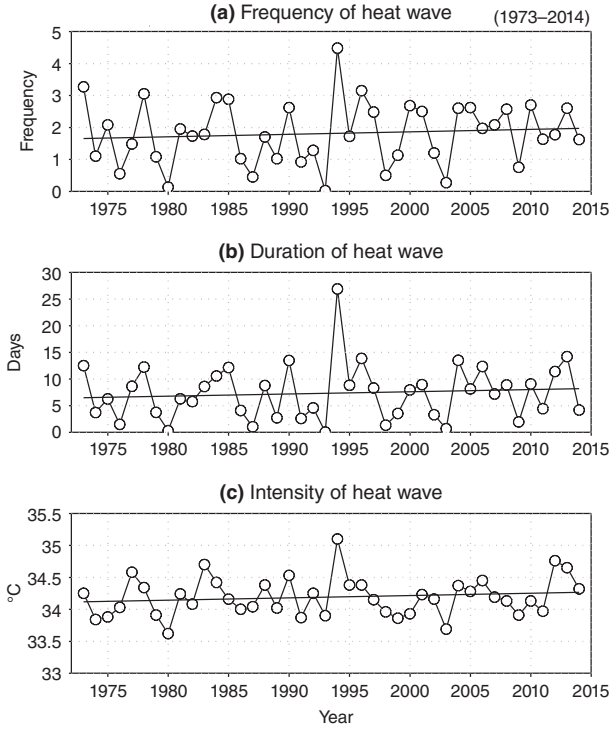

Figure 3. Yearly variations of (a) the heat wave frequency, (b) duration, and (c) intensity in South Korea. Nation-wide values are constructed for each index by summing the values over all 60 stations, respectively. See the text for the definitions.

past 42 years. Nationwide values are constructed for each index by aggregating values at each station over all 60 stations. All the time series exhibit substantial variation over the years, implying possible connections with large-scale climate variability in interannual timescale. A notable episode is the year 1994, when the frequency, duration, and intensity time series all exhibit the maxima among the 42 years. The severity of this episode and the dynamical mechanisms associated with large-scale upper-level atmospheric flow are discussed by Park and Schubert (1997). 2013 is the second only for the HWD (Figure 3(b)). Due to

Table 1. Temporal correlation among the heat wave indices in South Korea. The correlation coefficient was calculated based on yearly values for 42 years (1973–2014).

CC	Frequency	Intensity	Duration
Frequency	1	0.65	0.91
Intensity		1	0.82
Duration			1

a large amount of interannual variation, the secular trend is not statistically significant, although it is weakly positive in the three time series. As shown in Table 1, these indices show high time correlations with each other, suggesting that they are not independent but interrelated. We next investigate the spatial and temporal variability of heat waves in South Korea by applying the EOF analysis to the yearly values of HWF defined at each station, where our analysis is particularly focused on the interannual variation of HWF and its geographical distribution. Figure 4 shows the spatial patterns of the two leading eigenvectors and the corresponding PC time series. The first and the second modes (EOF1 and EOF2, respectively) account for 50.8 and 9.0% of the total variance, respectively. Remaining modes are less significant by explaining small percentage variance below 5%, and their spatial patterns are manifested by a lot of local features. Here only the two leading eigenvectors are discussed. The EOF1 (Figure 4(a)) exhibits one sign over the entire region in South Korea. The corresponding PC1 time series (Figure 4(b)) has no trend but with significant interannual variation. For example, the extremely above-normal occurrence of heat wave days in the summer of 1994 is quite evident.

The second mode (EOF2, Figure 4(c)) shows a see-saw pattern with two major centres of variability, one over the southeast and the other over the northwest. This spatial pattern corresponds to the PC time series (PC2, Figure 4(d)) that exhibits a much longer time scale variation with a clear trend. This suggests that the southeastern part of the peninsula has a signal of rapid increase of HWF since the mid-1990s, compared with the rest of the region.

Much of climate variability in interannual timescale is known to be related with the SST forcing in local and/or in remote (e.g. Min *et al.*, 2014). To examine the possible influence from the SST forcing, first we analyse the regression patterns of SST anomalies in global domain with PC1 (Figure 4(b)) and PC2 (Figure 4(d)), respectively, which results are presented in Figure 5. EOF1 is associated with the large-scale SST variability in summer (Figure 5(a)), with strong signal both in tropical and midlatitude oceans. The occurrence of heat wave days in Korea is largely associated with the SST increase in the mid-latitude western North Pacific, particularly in the oceans adjacent to Korea and Japan. The local SST increase may contribute to increase the hot days over land through increased oceanic heat flux to the atmosphere. On the other hand, the SST increase in midlatitudes can be regarded as a response to the change in large-scale atmospheric circulation. Indeed, Park and Schubert (1997) suggested that the midlatitude SST anomalies are primarily a response to the atmospheric forcing, as surmised by the lagged relationship of SST

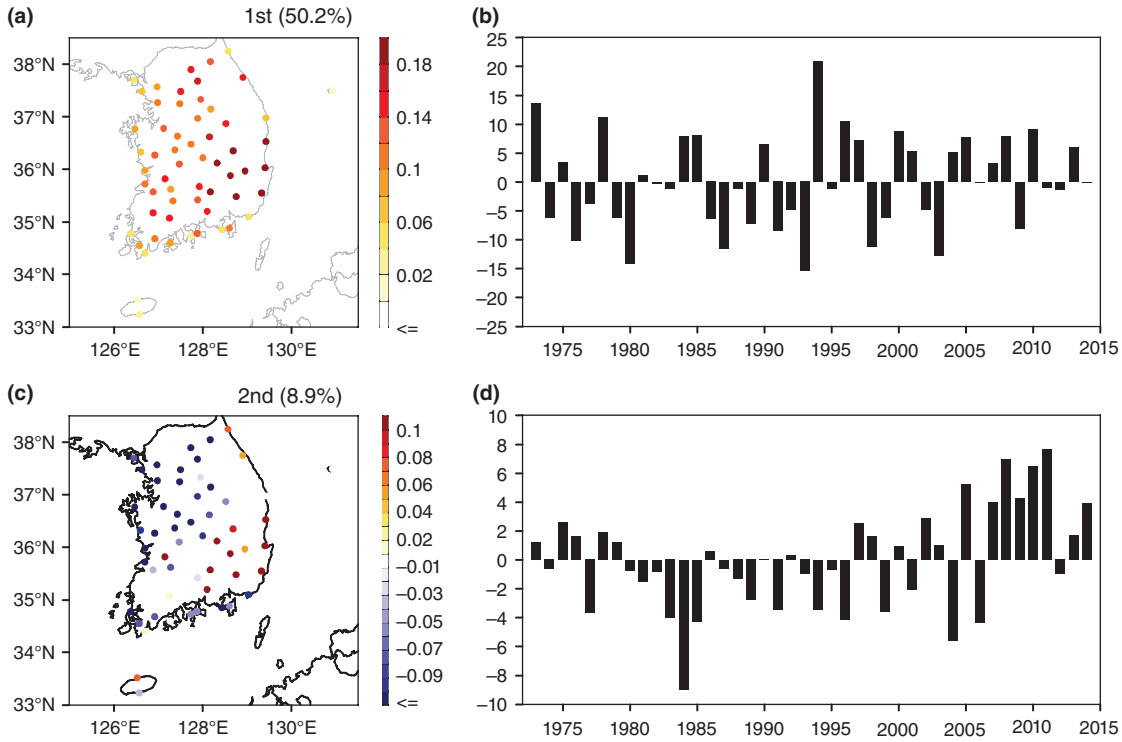

Figure 4. (a) Spatial pattern of the first empirical orthogonal function (EOF1) of the heat wave frequency and (b) the associated principal component time series (PC1). (c) and (d) are the spatial pattern of the second mode (EOF2) and the associated time series (PC2), respectively. These two leading modes explain 50.8 and 9.0% of the total variance, respectively.

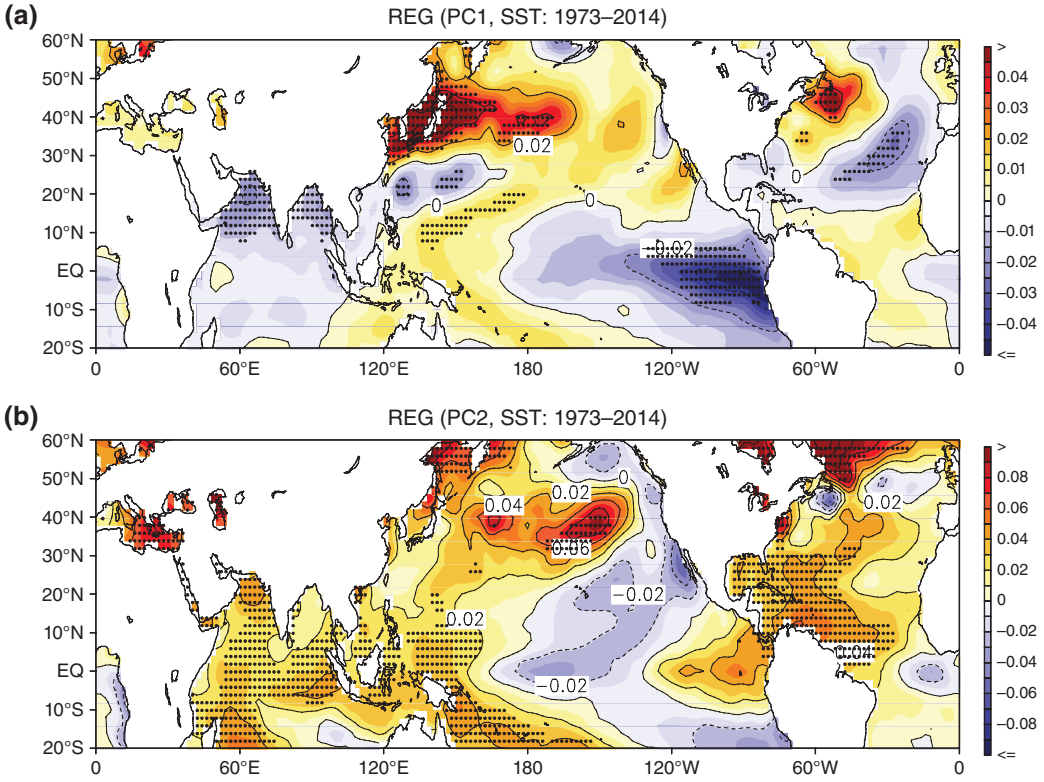

Figure 5. Regression pattern of the sea surface temperature (SST) anomalies (unit: K) related to (a) EOF1 and (b) EOF2. SST data were obtained from NOAA ERSST version 3.

with respect to the 500-hPa GPH anomalies. The heat wave days in summertime Korea are often accompanied by large-scale atmospheric subsidence with high pressure anomalies at surface. This process tends to induce a long spell of dry days with less cloud and precipitation, which can contribute to increase the SST. As will be discussed in the next subsection, the large-scale atmospheric circulation can be changed through teleconnections triggered by diabatic heating in the tropics. Over the Northwest Pacific, there is a hint of atmospheric teleconnection reflected in the SST anomalies. They produce a tripolar pattern with alternating signs northwards from the tropics to the midlatitudes, where the positive SST is in the equatorial western Pacific, negative in the South China Sea, and positive in the midlatitude oceans around Korea and Japan. The SST pattern associated with the Korean HWF also shows a strong signal over the equatorial eastern Pacific, the pronounced ENSO variability region. This supports the idea again that the yearly variation of HWF over Korea is largely explained by ENSO in the tropical oceans and associated atmospheric large-scale teleconnection pattern. The temporal correlation between two indices of HWF in Figure 3(a) and PC1 in Figure 4(b) is as high as 0.97, suggesting the PC1 as a representative index for describing interannual variation of Korean HWF. We use the PC1 for the rest of the analysis, although the results are quite similar when we replace the index with the one in Figure 3(a).

The SST anomaly pattern associated with EOF2 (Figure 5(b)) reflects the influence of SST on Korean HWF in much longer time scale. This pattern resembles the Pacific Decadal Oscillation (Mantua and Hare, 2002) or the secular trend pattern of global SST changes with a La Nina-like pattern (England *et al.*, 2014). At this time, it is rather unclear whether the long-term SST changes in the global oceans are able to drive a northwest-southeast see-saw pattern of the Korean HWF variability, or they merely reflect the resemblance of temporal scale just in a statistical sense, as the PC2 time series (Figure 4(d)) exhibit multi-decadal variation with a secular trend. Most of the tropical and midlatitude oceans in the Pacific show correlation with no statistical significance at 5% level. It seems less likely that this global long-term SST changes can drive the local see-saw pattern, and we exclude this variability mode for further discussion.

3.2. Connections with large-scale atmospheric circulation patterns

As the major mode of variability explaining the Korean HWF more than 50 % of the total, from now on we focus our analysis on the interannual variability associated with EOF1. To identify the dominant large-scale mechanisms engaged with Korean heat waves, we conducted the regression analysis between PC1 and large-scale atmospheric variables. Figure 6 shows the regression patterns of GPH at 500 hPa, 2-m temperature, SLP, the moisture convergence and moisture flux integrated vertically from surface to 300 hPa, and OLR, all projected onto the PC1 of Korean HWF. The regression analysis used the anomalies by removing seasonal cycle in each variable, and only the areas of statistical significance in the correlation at the

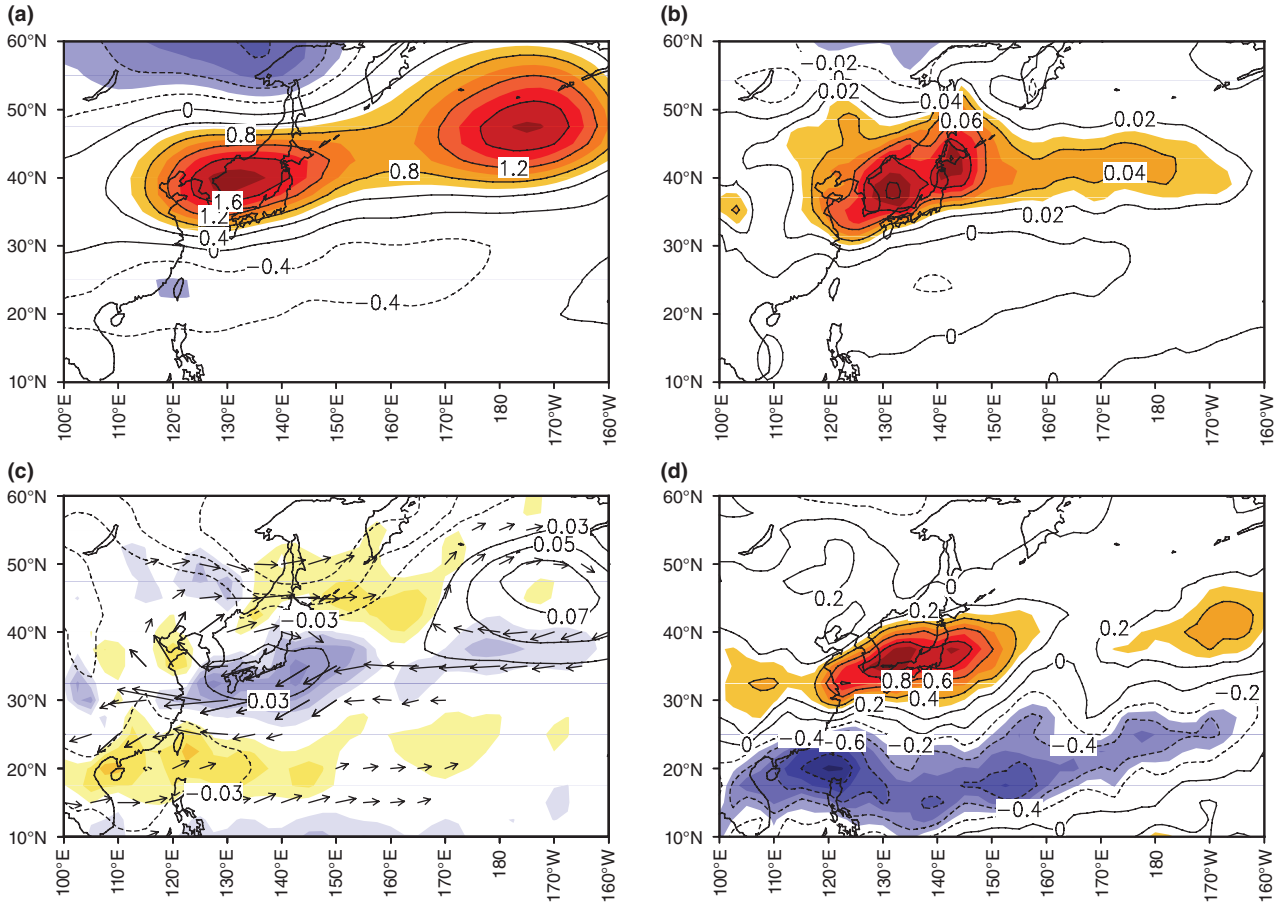

Figure 6. Regression patterns of (a) 500 hPa geopotential height (GPH in m), (b) 2-m temperature(°C), (c) sea level pressure (SLP in hPa, contour lines), vertically integrated moisture flux (g kg^{-1} m s^{-1}, vector) and moisture convergence (mm day^{-1}, shaded), and (d) outgoing longwave radiation (OLR) during July–August. All data were from the NCEP/NCAR-1 reanalysis except for OLR from NCEP CPC. Anomaly patterns are obtained by removing seasonal cycle in each variable and projected onto the PC1 time series of the Korean HWF. The shaded regions represent the area of exceeding the 95% confidence level from the Student's *t* test. For the vertically integrated moisture flux vector in (c), only those areas of exceeding the 95% confidence level are indicated.

95% confidence level (at $p < 0.05$) are shown in Figure 6. This confidence level is popularly used in the previous studies (e.g. Haylock and Goodess, 2004; Cassou *et al.*, 2005). The 500-hPa GPH anomaly (Figure 6(a)) shows a positive maximum over Korea and Japan, whose pattern is extended east and west. To the north and south are the zonally extended, negative minima of GPH anomalies, suggesting a hint of northward propagating teleconnection pattern in responding to the tropical diabatic heat source in the Northwest Pacific (Nitta, 1987; Wang *et al.*, 2001). The regression pattern of the 2-m temperature (Figure 6(b)) also shows a similar spatial structure, which corresponds to the positive GPH anomaly to an anomalous surface warming and the negative to a cooling, respectively. Although not shown, it is found that strong surface warming over Korea is accompanied by mid- to upper-level positive thickness anomalies, suggesting that the processes relevant with Korean heat waves are not just confined in low levels but connected with large-scale circulation changes from surface to upper levels. The pattern results in persistent subsidence and adiabatic warming with the increase of atmospheric stability, which can cause severe heat waves over Korea and Japan.

Figure 6(c) shows that the significant decrease of moisture convergence (shaded in warm colours) over Korea and Japan is associated with positive SLP anomalies in the region. On the other hand, the increase of moisture convergence and the negative SLP anomalies are located in one over the subtropical western Pacific and the South China Sea and another over Sakhalin in the Far Northeast Asia. The anticyclonic circulation anomalies associated with positive SLP anomalies over Northeast Asia are responsible for an insufficient supply of moisture from the tropical oceans (Wu and Chen, 2012), instead the moisture is transported towards East Asia to enhance the moisture convergence over a large region from off the east coast south China to east of 140°E. The OLR anomaly pattern in Figure 6(d) shows a strengthening of convection associated with increased moisture convergence over the South China Sea and the Northwest Pacific near 20°N, and a weakening of convection with decreased moisture convergence in Korea and Japan.

Figure 7(a) shows the correlation map between PC1 and relative vorticity at 150 hPa level, and Figure 7(b) the meridional and vertical cross-section of correlation between PC1 and atmospheric winds over 110–135°E.

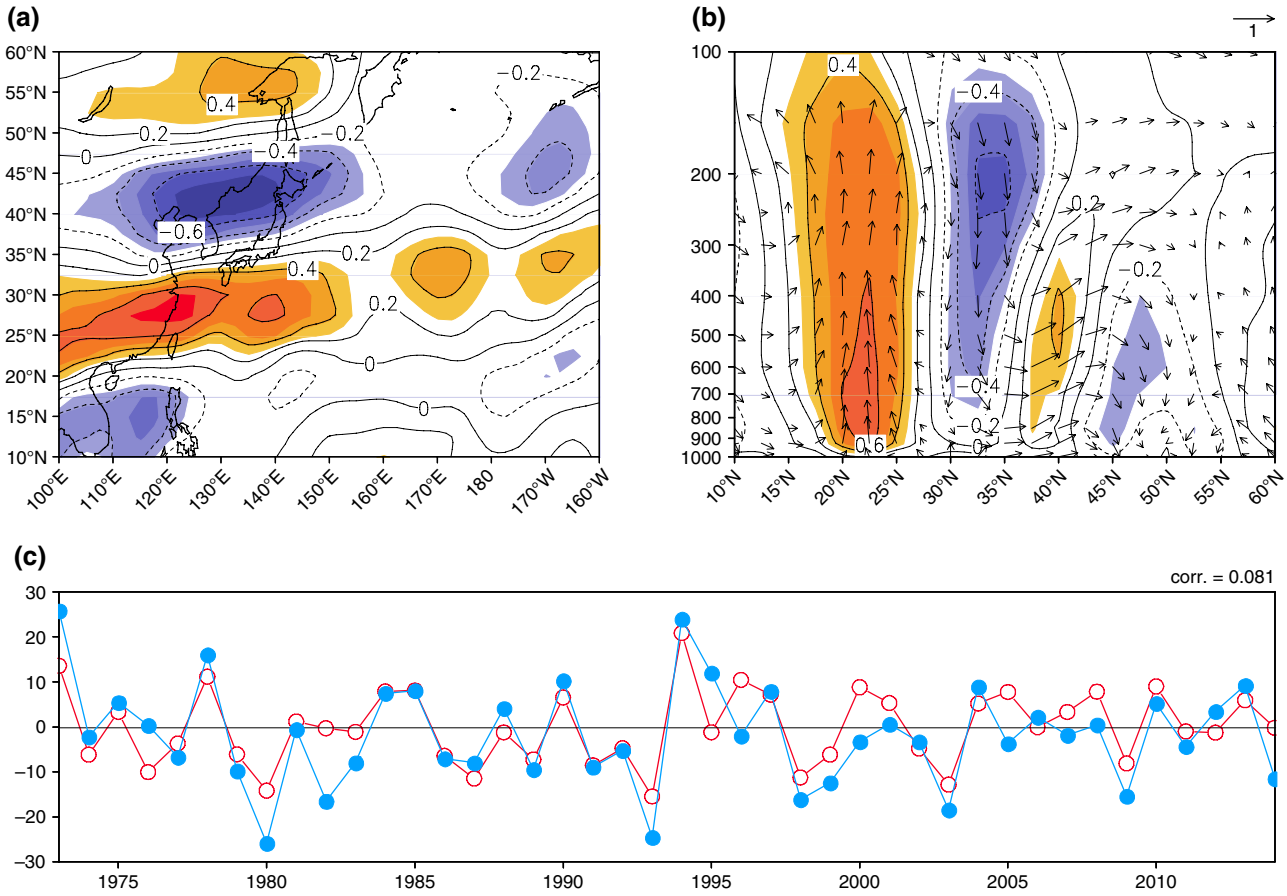

Figure 7. Correlation patterns between PC1 of the Korean HWF and (a) 150-hPa vorticity and (b) meridional-vertical circulation (vector) and vertical velocity (ω, shading, positive values indicate upward motion) over 110–135°E. (c) The time series of the PC1 (red open circle) from 1973 to 2014 and the vorticity difference at 150 hPa between the area of 25–30°N and 110–130°E and the area of 35–45°N and 120–140°E (blue closed circle). Shading in (a) and (b) indicates the areas of exceeding the 95% confidence level.

The intense moisture convergence and deep convection drives an upper-level positive vorticity (Figure 7(a)). The positive correlation of vorticity at 150 hPa in the East and South China Seas induces more convection and diabatic heating (Figure 6(d)), which becomes a source of Rossby wave train that drives negative vorticity anomaly around Korea, and alternating positive vorticity anomaly in the northeastern end of Asia and the Sea of Okhotsk. One of the notable features appeared in Korean heat waves is the clear barotropic structure in the vertical motion (Figure 7(b)), with significant anomalous convergence and upward motion in the Northwest Pacific and with anomalous divergence and downward motion in East Asia. The barotropic atmospheric response is typically for the Rossby-type waves in the teleconnection patterns (Wang *et al.*, 2001). The adiabatic atmospheric warming due to the anomalous downward motion seems to be a dominant mechanism responsible for heat waves in Korea during July to August. Note that vertical motion anomalies in Figure 7(b) show vertical tilting structure towards the pole particularly in the mid-latitudes, which feature is consistent well with the finding of Kosaka and Nakamura (2006) for the PJ teleconnection pattern. This vertical tilting tends to shift the centre of anticyclonic flow around Korea and Japan to the north in the upper level (Figure 7(a)) from the centre location appeared at sea level (Figure 6(c)).

Table 2. Correlation coefficients between the HWF PC1 time sires and the various monsoon indices defined by Wang and Fan (1999) (WF = U850(5°–15°N, 90°–130°E) – U850 (22.5°–32.5°N, 110°–140°E), Zhang *et al.* (2003) (Zh = U850 (10°–20°N, 100°–150°E) – U850(25°–35°N, 100°–150°E), and Wang *et al.* (2001) (EAM = V850(20°–30°N, 110°–140°E) – V850(30°–40°N, 110°–140°E), respectively. U850 and V850 denote the zonal and the meridional winds at 850 hPa, respectively. Also presented is the correlation coefficient between the HWI and the SST index averaged over the Niño 3.4 region (5°N–5°S, 120°–170°W). The correlation coefficient of 5% significance level is indicated in bold.

	WF(JA)	Zh(JA)	EAM(JA)	Nino3.4(JA)
PC1(1973–2014)	**0.35**	**0.40**	**0.42**	−0.20

Regarding the occurrence of Korean heat waves, two major centres of interannual variability are identified in the regression pattern of the upper-level vorticity in Figure 7(c). We designate the vorticity difference at 150-hPa level between the average over 25°–30°N, 110°–130°E and the average over 35°–45°N,

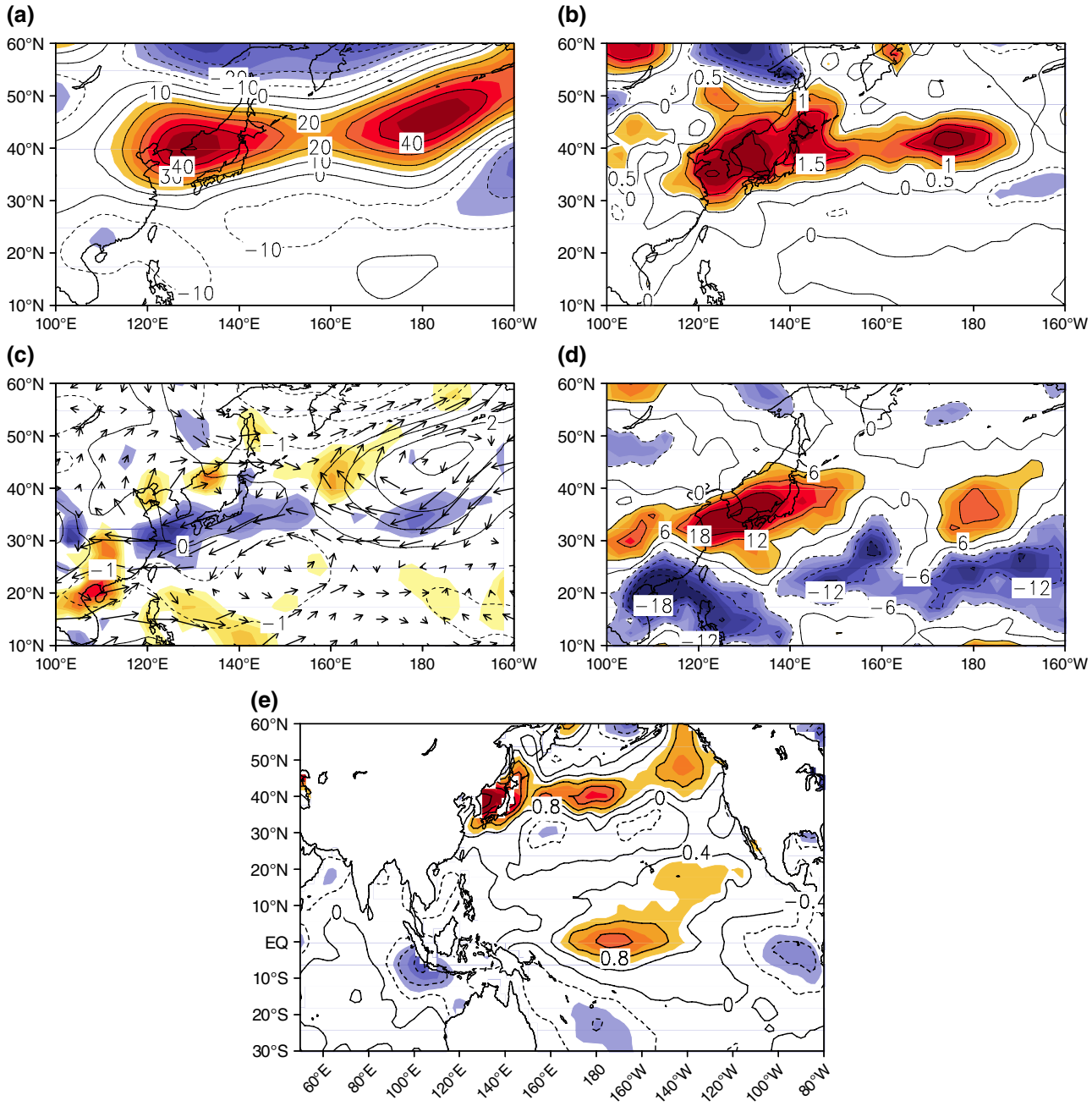

Figure 8. Anomaly patterns in July–August 1994 for (a) 500-hPa GPH (m), (b) 2-m temperature (°C), (c) SLP (hPa, contour lines), vertically integrated moisture flux (g kg^{-1} m s^{-1}, vectors), and moisture convergence(mm day^{-1}, shaded), (d) OLR (W m^{-2}), and (e) SST (°C).

120°–140°E as a favourable condition of Korean heat waves. The correlation between PC1 and the time series of vorticity difference reaches up to 0.81 with significance at the 95% confidence level by the Student's *t*-test. This suggests that the long-range prediction for the occurrence frequency of Korean heat waves is possible from the reliable prediction of large-scale upper level circulation.

We note that the large-scale circulation changes and convection associated with frequent occurrences of heat wave events in Korea are largely affected by the interannual variability of East Asia summer monsoon. The correlation coefficients between PC1 and various monsoon indices defined by Wang and Fan (1999), Wang *et al.* (2001), and Zhang *et al.* (2003) all show statistical significance (Table 2), in spite of minor differences in their definitions, suggesting that the strong monsoon over the western North Pacific tends to drive a more frequent occurrence of summertime hot days in Korea. In particular, the regression patterns shown in Figures 5–7 match quite well with those presented by Wang *et al.* (2001), where active (suppressed) convection over the western North Pacific tends to drive low-level cyclonic (anticyclonic) circulation anomalies and upward (downward) motion in the western North Pacific and the South China Sea, which it induces anti-cyclonic (cyclonic) circulation and downward (upward) motion in Korea and Japan. Together with the

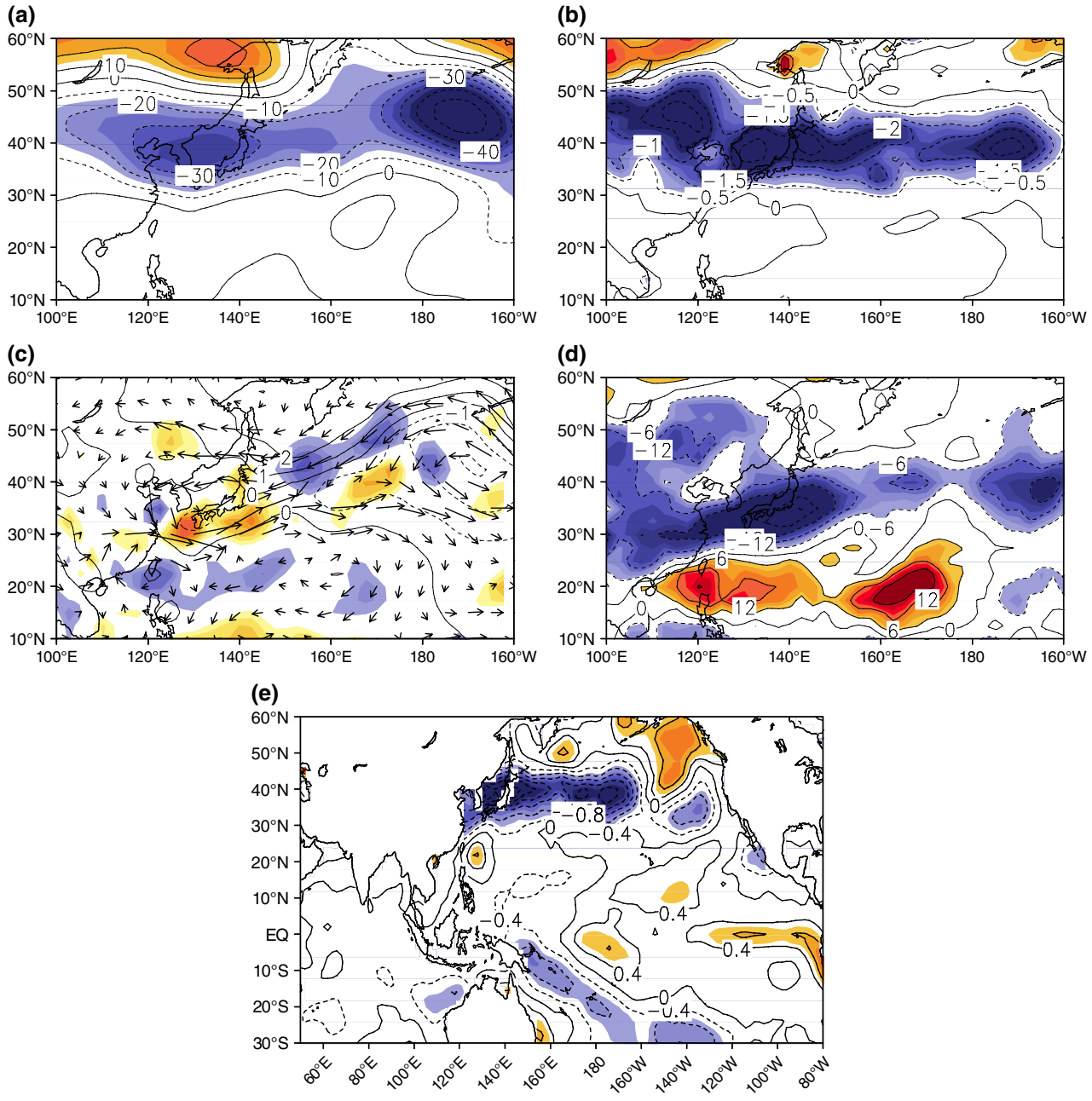

Figure 9. Anomaly patterns in July–August 1993 for (a) 500-hPa GPH (m), (b) 2-m temperature (°C), (c) SLP (hPa, contour lines), vertically integrated moisture flux (g kg^{-1} m s^{-1}, vectors), and moisture convergence(mm day^{-1}, shaded), (d) OLR (W m^{-2}), and (e) SST (°C).

cyclonic circulation anomalies to the further north, this tripolar circulation pattern is the signature of teleconnection response to the tropical monsoon precipitation and diabatic heating over the western North Pacific (c.f. Figure 12 in Wang *et al.*, 2001).

As mentioned early, the summer of 1994 was a record-breaking season with the most frequent heat wave events in South Korea for the past 42 years (See Figure 3). Figure 8 shows the large-scale circulation (Figure 8(a)–(d)) and SST (Figure 8(e)) anomalies in July–August 1994. These circulation anomalies are consistent well with the patterns shown in Figures 5 and 6, but with stronger amplitudes, suggesting that the large-scale atmospheric teleconnection is the dominant mechanism for this record-breaking year. Note that the case is quite opposite in 1993 when the occurrence frequency of heat wave events in South Korea was the least as appeared in Figure 3(a). Large-scale anomalies in 1993 (Figure 9) just reversed their sign from the case in 1994 (c.f. Figure 8), suggesting that the large-scale patterns identified from the regression analysis tend to explain well both the maximum and the minimum years.

On the other hand, some differences are found in the SST anomalies in 1994 (Figure 8(e)) from the typical patterns related with Korean heat waves shown in Figure 5. There existed SST warming in the equatorial Central Pacific in 1994, being contrary to the La Nina-like pattern appeared in the typical, above-normal heat wave years in Korea (as

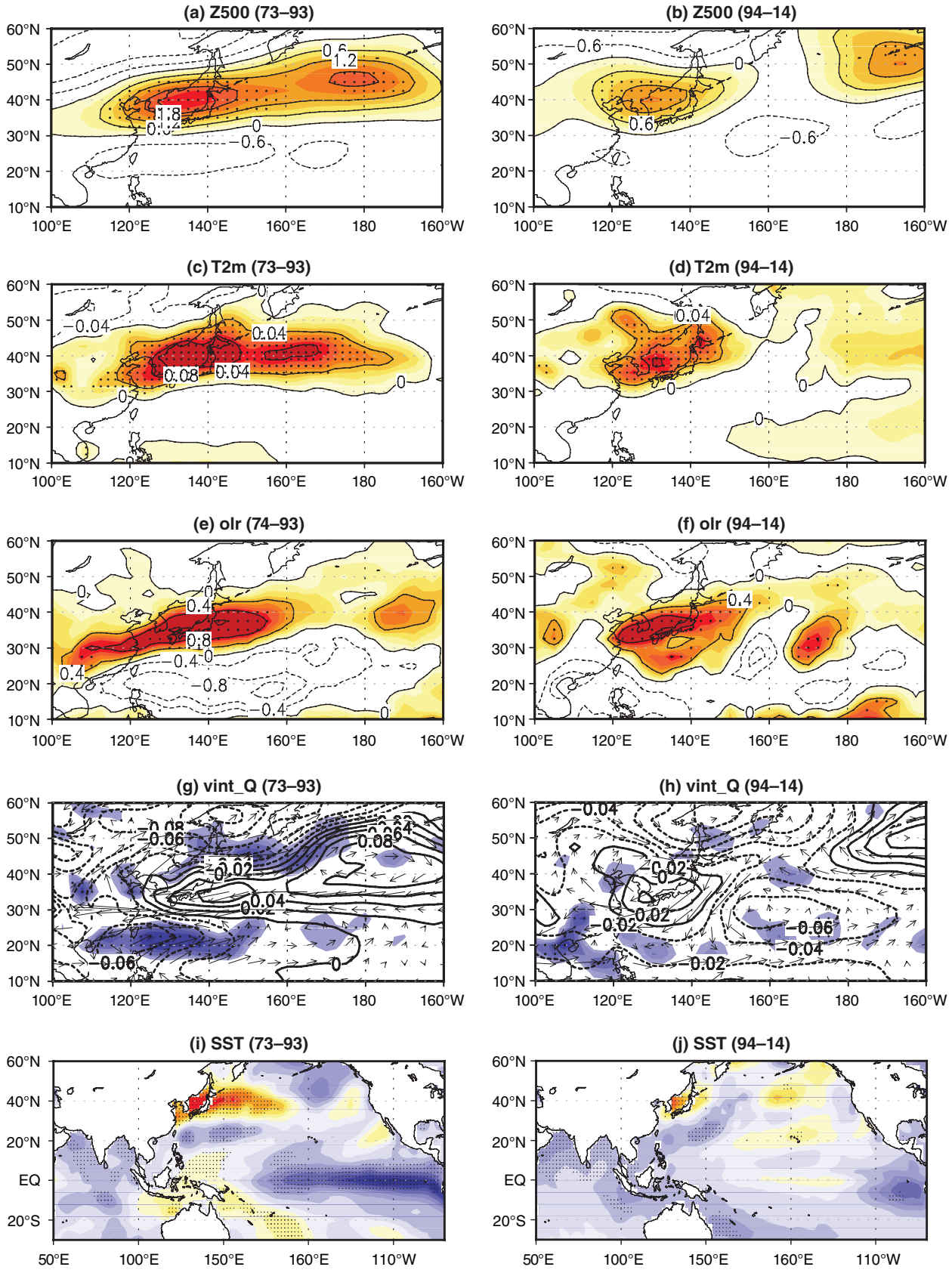

Figure 10. Regression patterns onto the PC1 of the Korean HWF. (a) and (b) are 500-hPa GPH anomalies (m), (c) and (d) 2-m temperature (°C), (e) and (f) OLR (W m^{-2}), (g) and (h) SLP (hPa, contoured lines), vertically integrated moisture flux (g kg^{-1} m s^{-1}, vector), and moisture convergence (mm day^{-1}, shaded), and (i) and (j) SST (°C) in 1973–1993 (left panels) and 1994–2014 (right), respectively. Grid points with statistical confidence levels exceeding 95% are indicated by closed circles in the figure. The PC1 time series were detrended in each period before the regression.

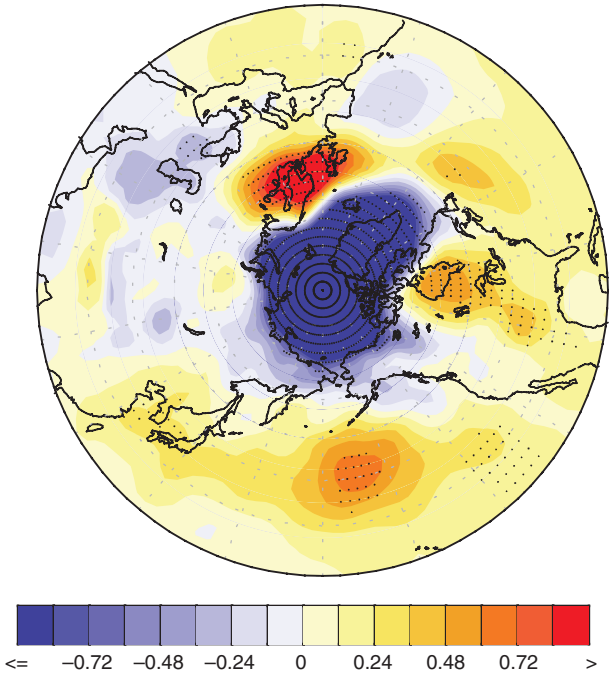

Figure 11. Regression pattern of SLP with the first EOF mode of the Arctic SLP variability (unit: hPa). The first mode accounts for 22.1% of the total variance when the EOF analysis was applied to the SLP field to the north of 60°N for 1973–2014. The NCEP/NCAR-1 reanalysis data were used, and the areas of the statistical confidence above 95% are indicated by closed circle.

shown in Figure 4(a)). This suggests that the large-scale atmospheric circulation patterns that drive the Korean heat waves are not always associated with the tropical ENSO, but with more complicating interaction between ENSO and East Asia monsoon that may initiate various diabatic forcing in the Indo-Pacific warm pool region. Indeed, the correlation between the Nino3.4 index and HWF is very low, with no statistical significance, showing weak relationship between the two. In addition, this low correlation is partly caused by even lower connection in the recent decade. This decadal change will be discussed in the next subsection.

The major heat wave year of 1994 (Figure 8(e)) and the minimum year of 1993 (Figure 9(e)) were both accompanied by large SST anomalies in the mid-latitude oceans near Korea, Japan, and northwestern Pacific. In a similar analysis, Min *et al.* (2014) also found that heat wave events in Korea are mostly associated with the summertime SST increase in the region. At this time, it is unclear whether these warm SST anomalies triggered this major heat wave year, or they are the response to the persistent large-scale subsidence, although the study of Park and Schubert (1997) showed that atmospheric forcing leads the anomalous SST patterns in a few weeks in the central North Pacific.

3.3. Decadal changes in atmospheric circulations

In this section, we examine further whether the large-scale forcing mechanism for heat waves in Korea has long-term changes, by separating analysis periods into 1973–1993 and 1994–2014. The decadal shift of the climate variability in the mid-1990s has been identified by many previous literatures (such as Kwon *et al.*, 2005, 2007; Yim *et al.*, 2008, 2013; Kajikawa *et al.*, 2009; Yeh *et al.*, 2010; Kang *et al.*, 2014b, and many). It is noted that separation before and after 1994 was trivial so that the inclusion or removal of 1994 did not significantly alter the regression patterns. It is also noted that the Korean HWF time series (PC1 in Figure 4) were detrended in each period to avoid any unnecessary influence by temporal trend, although the results were almost identical between the trended and detrended analyses. Figure 10 compares the regression patterns of PC1 with large-scale circulation fields and SST. A notable difference is a weaker relationship between the Korean HWF and large-scale circulation anomalies in the recent decades. The amplitudes of regressed anomalies are decreasing, and with more contracted patterns around Korea and Japan. This suggests a weakened PJ teleconnection pattern in the recent. This is somewhat intriguing because the weakened atmospheric teleconnection might lead to the decrease of HWF in Korea. However, there is no clear sign of decrease in the HWF time series (Figure 3). Although there is no satisfactory explanation to this change yet, one cannot exclude the influence of global warming and a significant increase of summertime-mean temperature in recent years (Min *et al.*, 2014).

Another possible scenario is the long-term changes in the large-scale atmospheric teleconnection patterns relevant with the Korean heat waves. Recently, Tang *et al.* (2014) suggested that recent polar warming and the Arctic ice melting might cause the increase of summer-mean temperature and more frequent occurrence of heat waves in the Northern Hemisphere. In their mechanisms, the decrease of sea ice extent tends to drive the weakening and poleward shift of the upper-level jet stream. This tends to excite and maintain persistent, large-scale atmospheric waves and long-term hot spells.

To explore the possible linkage between Korean heat wave events and the Arctic, we first extracted the indices that represent the interannual variability in the Arctic by applying EOF analysis to the SLP field north to 60°N. The first mode of July–August mean SLP variability accounts for 22.1% of the total variability, which is known as the summertime AO (Thompson and Wallace, 1998). This pattern is featured by zonally symmetric annular mode with pressure variation between the Arctic and the high latitudes, as shown in Figure 11, the regression pattern of SLP over the Northern Hemisphere. The SLP regression pattern associated with AO also highlights the linkage in East Asia including South Korea and Japan. Associated PC time series with the first EOF (Figure 12, blue line; hereafter referred to the AO index) exhibits a significant interannual variation.

In Figure 12, we compare three time series for the period of 1973–2014: the Korean HWF PC1, the Nino3.4 index, and the AO index, and the temporal correlations between the time series are shown in Table 3. The correlations become statistically significant in the recent decades (1994–2014), suggesting an enhanced relationship

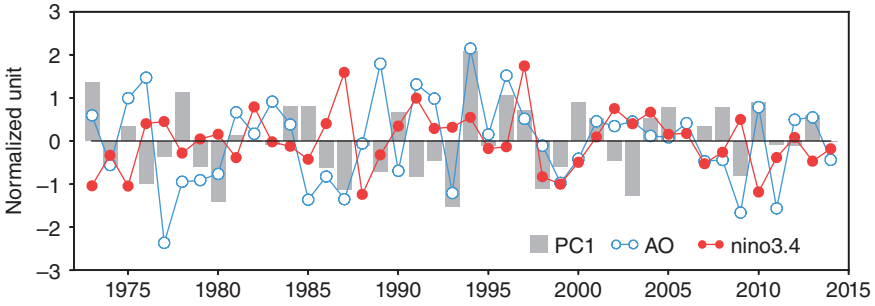

Figure 12. Time series of the Korean HWF PC1 (grey bars), the AO index (line with open circle), and the Nino 3.4 index (line with filled circle) for July–August. The trend is removed and the temporal variation is normalized in each time series. The sign of the Nino 3.4 index is reversed from the original.

Table 3. Correlation coefficients between the HWF PC1 time series and the AO and the NINO3.4 indices, respectively. The numbers in parentheses show the correlation coefficients with the detrended time series. The correlation coefficient of 1% significance level is indicated in bold.

	1973–2014	1973–1993	1994–2014
AO	0.26(0.28)	0.06(0.04)	**0.54 (0.56)**
Nino3.4	−0.20(−0.22)	**−0.55(−0.53)**	0.04(0.09)

between the Arctic climate variability and East Asia. The correlation is quite low in the past decades of 1973–1993. This is quite contrary to the case of ENSO, where the strong, negative correlation between ENSO and the Korean HWF for 1973–1993 has turned into no significant correlation for 1994–2014. This suggests that dominant mechanisms that drive the heat wave episodes in Korea and East Asia have changed, from the tropical forcing in the past decades to the Arctic forcing in the recent decades.

Figure 13 compares the six regression patterns of the 200-hPa zonal wind anomalies onto the Korean HWF index (Figure 13(a) and (b)), the AO index (Figure 13(c) and (d)), and the Nino3.4 index (Figure 13(e) and (f)), respectively for the two separate periods of 1973–1993 and 1994–2014. During the former period of 1973–1993, meridionally propagating wave pattern from the subtropical Northwest Pacific to Eurasia is prominently associated with the Korean heat waves (Figure 11(a)), implying significant influence from the tropical convection and diabatic heat source. This pattern is basically corresponding with those presented in Figures 6(a) and 7(a) at 500 hPa, where the former shows more zonally elongated pattern. Note that the regression pattern onto the Korean HWF (Figure 13(a)) shows much resemblance to that onto the Nino3.4 index (Figure 13(e)), particularly in East Asia during 1973–1993, suggesting a more dominant role by ENSO in modulating Korean HWF. On the other hand, the magnitude of upper-level wind anomalies associated with ENSO decreases substantially with no statistical significance in East Asia during 1994–2014 (Figure 13(f)), suggesting ENSO plays no significant role in modulating Korean heat waves. The regression pattern projected onto the AO index during the period of 1973–1993 (Figure 13(c)) shows the large-scale upper-level response associated with AO, but the signal is weak and not statistically significant in East Asia. This signal becomes stronger and statistically significant during the period of 1994–2014 (Figure 13(d)). Much resemblance in the spatial pattern between Figure 13(b) and (d) suggests that the influence by the Arctic on the development of Korean heat waves becomes as a more important mechanism in the recent decades. Although the regression patterns are superimposed by high wavenumber disturbances, they are more or less zonally symmetric. In Northeast Asia, the positive AO tends to make the circumpolar vortex stronger and more compact in the Arctic, and thereby shifting the location of subtropical jet further north. Persistent high pressure anomalies can intensify the occurrence of hot days and major heat waves in the region. We note that the proposed mechanism of the heat wave development by jet stream movement is entirely different from that suggested by Tang *et al.* (2014) who speculated the shift of the jet stream to north in the negative phase of AO. This is not the case in our investigation, and the positive phase of AO tends to drive the enhancement and northward shift of the jet stream.

4. Summary

This study investigates the interannual variation of the HWF in South Korea over the past 42 years (1973–2014). Daily maximum temperature higher than 33 °C is used as a threshold for the extreme heat wave day, and at least two consecutive days that meet this criterion is defined as the heat wave. The yearly number of heat wave days from July to August each year at each station is defined as the HWF. Then, the EOF analysis is applied to this data to obtain the leading spatial pattern (EOF1) and associated time series (PC1) of the interannual variation of Korean heat waves. The EOF1 explains more than 50% of the interannual variability of HWF, which has the same sign over the entire South Korea. This suggests that heat waves in Korea tend to occur typically in larger spatial scale than the nation, being more influenced by large-scale atmospheric circulation pattern changes rather than local changes. The corresponding PC1 shows no significant trend, but with slightly more chance of heat waves in recent years after mid-1990s.

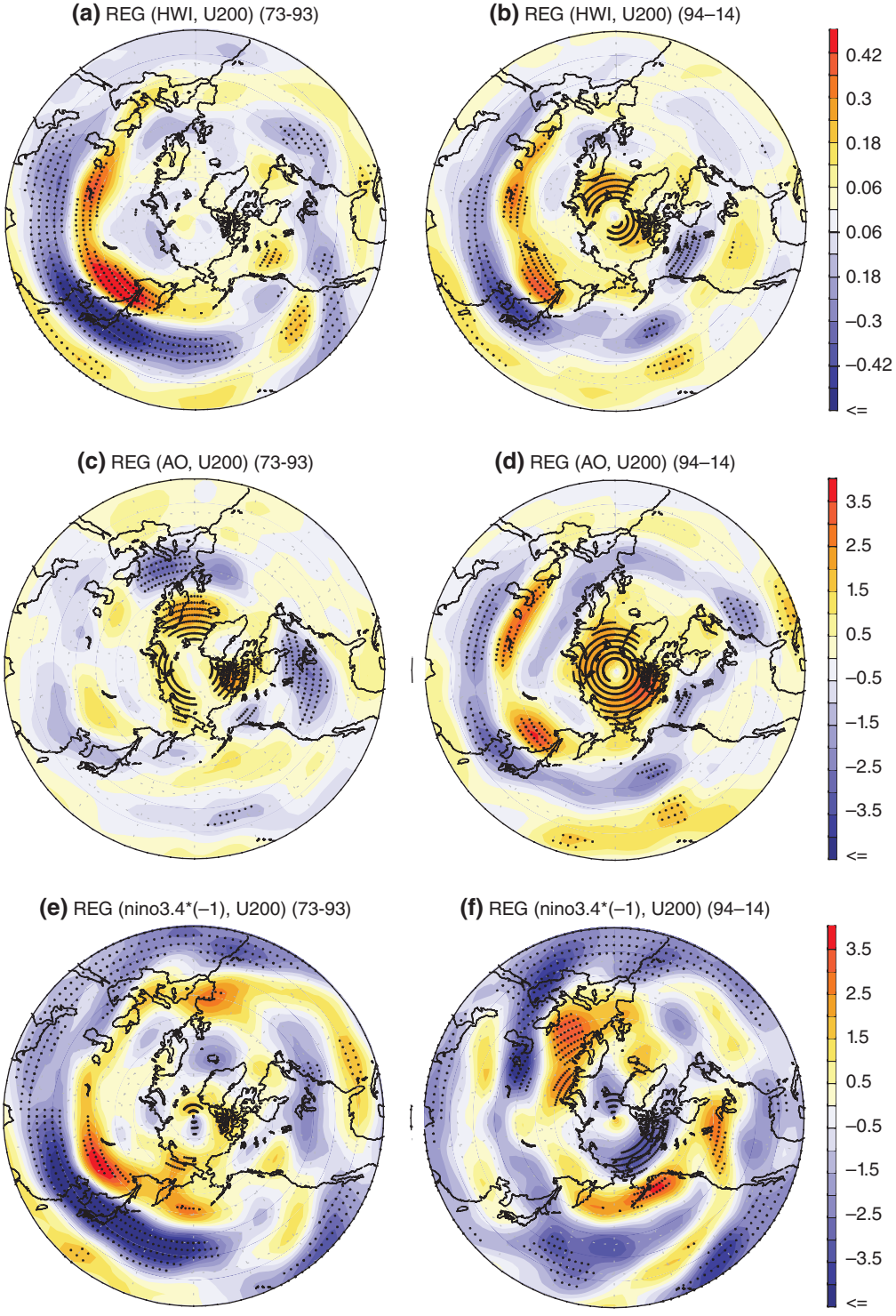

Figure 13. Regression patterns of 200-hPa zonal wind anomalies (unit: m s^{-1}) onto the Korean HWF PC1 time series during the periods of (a) 1973–1993 and (b) 1994–2014, respectively. (c) and (d) are same as in (a) and (b) except the regression onto the AO index, and (e) and (f) onto the Nino3.4 index. The temporal trends in the PC1 time series, the AO index and the Nino3.4 index were removed before regression. Areas of the statistical confidence above 95% are indicated by closed circle.

The regression of PC1 time series of the Korean HWF with large-scale atmospheric variables from the reanalysis data highlights the dynamical mechanisms that drive the heat waves. A noteworthy feature is the meridionally propagating pattern with the major centres of variability in the South China Sea and the Northwest Pacific, and another in East Asia around Korea and Japan in opposite sign. The positive correlation of vorticity at 150 hPa in the South and East China Seas indicates more convection and diabatic heating, which in turn becomes a source of Rossby wave-train that generates positive GPH anomalies around Korea and Japan. It is suggested that the Rossby waves are generated by the tropical heat source with positive correlation of vorticity over South China during

July–August. As a part of the propagating waves over East Asia, the adiabatic atmospheric warming due to the anomalous downward motion is dominant over Korea, which can be responsible for the severe heat wave events. The teleconnection pattern exhibits a clear barotropic structure in the vertical motion, which is typically for the Rossby wave response to the tropical forcing (Wang *et al.*, 2001).

A positive correlation between the cyclonic circulation over southern China and the East China Sea and the Korean heat waves are identified in the teleconnection pattern. This circulation change facilitates the convective activity in the southern China and the East China Sea, whereas it provides a condition of weakening moisture transport from the South China Sea and the Northwest Pacific to East Asia. An anomalous meridional circulation is associated with the anomalous downward motion over tropical oceans and the anomalous ascending motion near 20°N. It further leads to a descending motion in the mid-latitudes over Korea and Japan near 30–35°N. The associated downdraft tends to induce adiabatic warming and drying with reduced precipitation and total cloud amount. Therefore, the maximum temperatures at surface are tends to rise, causing extreme (hot and dry) weathers over Korea.

The dipole pattern appeared in upper-level vorticity between the active (inactive) convection area over the East China Sea and the inactive (active) convection area over East Asia in the case of more (less) frequent heat waves in Korea is explored to find a favourable large-scale condition for Korean heat waves. The vorticity difference index shows a significantly high correlation ($r = 0.81$). Further research effort is required to examine whether one can obtain a significant prediction skill for the index, using either statistical or dynamical methods.

This study also highlights that the driving mechanisms of heat waves in Korea and the adjacent East Asian region have shown significant changes in a decadal time scale. The aforementioned large-scale teleconnection pattern becomes weaker and the persistent high pressure pattern over Korea and heat wave days are more associated with the Arctic SLP variability in the recent decades after mid-1990s. This suggests that the relationship between Korean heat waves and tropical forcing tends to be weakened, while the influence from the Arctic becomes more enhanced. A more in-depth study is required to understand the dynamical and physical mechanisms on how the AO affects the development of heat waves in Korea and East Asia, including a numerical model experiment with varying diabatic heat source location.

Acknowledgements

This research was supported by the APEC Climate Center. ML was supported by the National Research Foundation of Korea (NRF) Grant funded by the Korean Government (MSIP) (No. NRF-2015R1A5A7037825).

References

Alexander L. 2011. Extreme heat rooted in dry soils. *Nat. Geosci.* **4**: 12–13, doi: 10.1038/ngeo1045.

Cassou C, Terray L, Phillips AS. 2005. Tropical Atlantic influence on European heat waves. *J. Clim.* **18**: 2805–2811.

Chen P, Newman M. 1998. Rossby wave propagation and the rapid development of upper-level anomalous anticyclones during the 1988 US drought. *J. Clim.* **11**: 2491–2504.

Choi KS, Wang B, Kim DW. 2012. Changma onset definition in Korea using the available water resources index and its relation to the Antarctic oscillation. *Clim. Dyn.* **38**: 547–562.

Christidis N, Stott P, Brown S, Hegerl G, Caesar J. 2005. Detection of changes in temperature extremes during the second half of the 20th century. *Geophys. Res. Lett.* **32**: L20716, doi: 10.1029/2005GL023885.

Coumou D, Rahmstorf S. 2012. A decade of weather extremes. *Nat. Clim. Change* **2**: 491–496, doi: 10.1038/NCLIMATE1452.

Coumou D, Robinson A. 2013. Historic and future increase in the global land area affected by monthly heat extremes. *Environ. Res. Lett.* **8**: 034018.

Dai AG, Trenberth KE, Karl TR. 1998. Global variations in droughts and wet spells: 1900–1995. *Geophys. Res. Lett.* **25**: 3367–3370, doi: 10.1029/98GL52511.

Ding Q, Wang B. 2005. Circumglobal teleconnection in the Northern Hemisphere summer. *J. Clim.* **18**: 3483–3505.

Ding Q, Wang B, Wallace JM, Branstator G. 2011. Tropical-extratropical teleconnections in boreal summer: observed interannual variability. *J. Clim.* **24**: 1878–1896.

Easterling DR, Meehl GA, Parmesan C, Changnon SA, Karl TR, Mearns LO. 2000. Climate extremes: observations, modelling, and impacts. *Science* **289**: 2068–2074.

England MH, McGregor S, Spence P, Meehl GA, Timmermann A, Cai W, Gupta AS, McPhaden MJ, Purich A, Santoso A. 2014. Recent intensification of wind-driven circulation in the Pacific and the ongoing warming hiatus. *Nat. Clim. Change* **4**(3): 222–227.

Hansen J, Sato M, Ruedy R. 2012. Perception of climate change. *Proc. Natl. Acad. Sci.* **109**: E2415–E2423.

Haylock MR, Goodess CM. 2004. Interannual variability of European winter rainfall and links with mean large-scale circulation. *Int. J. Climatol.* **24**: 759–777.

Hirschi MS, Seneviratne I, Alexandrov V, Boberg F, Boroneant C, Christensen OB, Formayer H, Orlowsky B, Stepanek P. 2010. Observational evidence for soil-moisture impact on hot extremes in southeastern Europe. *Nat. Geosci.* **4**(1): 17–21.

IPCC. 2013. *Climate Change 2013: The Physical Science Basis. Contribution of Working Group I to the Fifth Assessment Report of the Intergovernmental Panel on Climate Change*, Stocker TF, Qin D, Plattner G-K, Tignor M, Allen SK, Boschung J, Nauels A, Xia Y, Bex V, Midgley PM (eds). Cambridge University Press: Cambridge, UK and New York, NY, 1535 pp, doi: 10.1017/CBO9781107415324.

Kajikawa Y, Yasunari T, Wang B. 2009. Decadal change in intraseasonal variability over the South China Sea. *Geophys. Res. Lett.* **36**: L06810.

Kalnay E, Kanamitsu M, Kistler R, Collins W, Deaven D, Gandin L, Iredell M, Saha S, White G, Woollen J, Zhu Y, Chelliah M, Ebisuzaki W, Higgins W, Janowiak J, Mo KC, Ropelewski C, Wang J, Leetmaa A, Reynolds R, Jenne R, Joseph D. 1996. The NCEP/NCAR 40-year reanalysis project. *Bull. Am. Meteorol. Soc.* **77**: 437–471.

Kang D, Im J, Lee MI, Quackenbush LJ. 2014a. The MODIS ice surface temperature product as an indicator of sea ice minimum over the Arctic Ocean. *Remote Sens. Environ.* **152**: 99–108.

Kang D, Lee MI, Im J, Kim D, Kim HM, Kang HS, Schubert SD, Arribas A, MacLachlan C. 2014b. Prediction of the Arctic Oscillation in boreal winter by dynamical seasonal forecasting systems. *Geophys. Res. Lett.* **41**: 3577–3585.

Kenyon J, Hegerl GC. 2008. Influence of modes of climate variability on global temperature extremes. *J. Clim.* **21**: 3872–3889.

Kosaka Y, Nakamura H. 2006. Structure and dynamics of the summertime Pacific–Japan teleconnection pattern. *J. Meteorol. Soc. Jpn.* **132**: 2009–2030.

Kwon MH, Jhun JG, Wang B, An SI, Kug JS. 2005. Decadal change in relationship between east Asian and WNP summer monsoons. *Geophys. Res. Lett.* **32**: L16709, doi: 10.1029/2005GL023026.

Kwon MH, Jhun JG, Ha KJ. 2007. Decadal change in east Asian summer monsoon circulation in the mid-1990s. *Geophys. Res. Lett.* **34**: L21706, doi: 10.1029/2007GL031977.

Kysely J, Kim J. 2009. Mortality during heat waves in South Korea, 1991–2005: how exceptional was the 1994 heat wave? *Clim. Res.* **38**: 105–116.

Lee JY, Wang B, Wheeler M, Fu X, Waliser D, Kang IS. 2013. Real-time multivariate indices for the boreal summer intraseasonal oscillation over the Asian summer monsoon region. *Clim. Dyn.* **40**: 493–509, doi: 10.1007/s00382-012-1544-4.

Li S, Lu J, Huang G, Hu K. 2008. Tropical Indian Ocean basin warming and East Asian summer monsoon: a multiple AGCM study. *J. Clim.* **21**: 6080–6088.

Lindsay R, Wensnahan M, Schweiger A, Zhang J. 2014. Evaluation of seven different atmospheric reanalysis products in the Arctic. *J. Clim.* **27**: 2588–2606.

Mantua NJ, Hare SR. 2002. The Pacific decadal oscillation. *J. Oceanogr.* **58**: 35–44.

Meehl GA, Tebaldi C. 2004. More intense, more frequent and longer heat waves in the 21st century. *Science* **305**: 994–997.

Min SK, Kim YH, Kim MK, Park C. 2014. Assessing human contribution to the summer 2013 Korean heat wave [In "Explaining extreme events of 2013 from a climate perspective"]. *Bull. Am. Meteorol. Soc.* **95**(9): S48–S51.

Moon JY, Wang B, Ha KJ, Lee JY. 2013. Teleconnections associated with Northern Hemisphere summer monsoon intraseasonal oscillation. *Clim. Dyn.* **40**: 2761–2774.

Nakamura H, Fukamachi T. 2004. Evolution and dynamics of summertime blocking over the Far East and the associated surface Okhotsk high. *Q. J. R. Meteorol. Soc.* **130**: 1213–1234.

Nitta T. 1987. Convective activities in the tropical western Pacific and their impact on the northern hemisphere summer circulation. *J. Meteorol. Soc. Jpn.* **65**: 373–390.

Park CK, Schubert SD. 1997. On the nature of the 1994 East Asian drought. *J. Clim.* **10**: 1056–1070.

Scaife AA, Folland CK, Alexander LV, Moberg A, Knight JR. 2008. European climate extremes and the North Atlantic Oscillation. *J. Clim.* **21**: 72–83.

Schubert SD, Wang H, Suarez MJ. 2011. Warm season subseasonal variability and climate extremes in the Northern Hemisphere: the role of stationary Rossby waves. *J. Clim.* **24**(18): 4773–4792.

Serreze MC, Holland MM, Stroeve J. 2007. Perspectives on the Arctic's shrinking sea-ice cover. *Science* **315**: 1533–1536.

Smith TM, Reynolds RW, Peterson TC, Lawrimore J. 2008. Improvements NOAAs historical merged land–ocean temp analysis (1880–2006). *J. Clim.* **21**: 2283–2296.

Stroeve JC, Serreze MC, Holland MM, Kay JE, Maslanik J, Barrett AP. 2012. The Arctic's rapidly shrinking sea ice cover: a research synthesis. *Clim. Change* **110**: 1005–1027.

Sturaro G. 2003. A closer look at the climatological discontinuities present in the NCEP/NCAR reanalysis temperature due to the introduction of satellite data. *Clim. Dyn.* **21**: 309–316.

Tang Q, Zhang X, Francis JA. 2014. Extreme summer weather in northern mid-latitudes linked to a vanishing cryosphere. *Nat. Clim. Change* **4**: 45–50, doi: 10.1038/NCLIMATE2065.

Teng H, Branstator G, Wang H, Meehl GA, Washington WM. 2013. Probability of US heat waves affected by a subseasonal planetary wave pattern. *Nat. Geosci.* **6**(12): 1056–1061.

Thompson DW, Wallace JM. 1998. The Arctic Oscillation signature in the wintertime geopotential height and temperature fields. *Geophys. Res. Lett.* **25**(9): 1297–1300.

Trenberth KE, Stepaniak DP, Caron JM. 2002. Interannual variations in the atmospheric heat budget. *Geophys. Res. Lett.* **107**: D8, doi: 10.1029/2000D000297.

Wang B, Fan Z. 1999. Choice of South Asian summer monsoon indices. *Bull. Am. Meteorol. Soc.* **80**(4): 629–638.

Wang B, Wu R, Lau KM. 2001. Interannual variability of the Asian summer monsoon: contrasts between the Indian and the Western North Pacific–East Asian monsoons. *J. Clim.* **14**: 4073–4090.

Wang B, Lee JY, Kang IS, Shukla J, Park CK, Kumar A, Schemm J, Cocke S, Kug JS, Luo JJ, Zhou T, Wang B, Fu X, Yun WT, Alves O, Jin E, Kinter J, Kirtman B, Krishnamurti T, Lau N, Lau W, Liu P, Pegion P, Rosati T,Schubert S, Stern W, Suarez M, Yamagata T. 2009. Advance and prospectus of seasonal prediction: assessment of the APCC/CliPAS 14-model ensemble retrospective seasonal prediction (1980–2004). *Clim. Dyn.* **33**: 93–117.

Watanabe M, Shiogama H, Imada Y, Mori M, Ishii M, Kimoto M. 2013. Event attribution of the August 2010 Russian heat wave. *SOLA* **9**: 65–68.

Wen QH, Zhang X, Xu Y, Wang B. 2013. Detecting human influence on extreme temperatures in China. *Geophys. Res. Lett.* **40**: 1171–1176.

World Meteorological Organization. 2011. Weather extremes in a changing climate: hindsight on foresight. WMO Publication No. 1075, Geneva, Switzerland.

Wu W, Chen JL. 2012. Sensitivity of tropical cyclone precipitation to atmospheric moisture content: case study of Bilis (2006). *Atmos. Oceanic Sci. Lett.* **5**(5): 420–425.

Wu B, Zhou T, Li T. 2009. Seasonally evolving dominant interannual variability modes of East Asian climate. *J. Clim.* **22**(11): 2992–3005.

Yang J, Liu Q, Xie SP, Liu Z, Wu L. 2007. Impact of the Indian Ocean SST basin mode on the Asian summer monsoon. *Geophys. Res. Lett.* **34**: L02708, doi: 10.1029/2006GL028571.

Yeh SW, Kang SK, Kirtman BP, Kim JH, Kwon MH, Kim CH. 2010. Decadal change in relationship between western North Pacific tropical cyclone frequency and the tropical Pacific SST. *Meteorog. Atmos. Phys.* **106**: 179–189.

Yim SY, Jhun JG, Yeh SW. 2008. Decadal change in the relationship between east Asian–western North Pacific summer monsoons and ENSO in the mid-1990s. *Geophys. Res. Lett.* **35**: L20711, doi: 10.1029/2008GL035751.

Yim SY, Wang B, Kwon MH. 2013. Interdecadal change of the controlling mechanisms for East Asian early summer rainfall variation around the mid-1990s. *Clim. Dyn.* **42**: 1325–1333, doi: 10.1007/s00382-013-1760-6.

Zhang Q, Tao S, Chen L. 2003. The interannual variability of East Asian summer monsoon indices and its association with the pattern of general circulation over East Asia. *Acta Meteorol. Sin.* **61**: 559–568.